

# EXPERIMENTAL VALIDATION OF A MARINE PROPELLER THRUST ESTIMATION SCHEME

Luca Pivano\* Øyvind N. Smogeli\*\*  
Thor Inge Fossen\* Tor Arne Johansen\*

\* *Department of Engineering Cybernetics, Norwegian University of Science and Technology, Trondheim, Norway*  
\*\* *Department of Marine Technology, Norwegian University of Science and Technology, Trondheim, Norway.*

Abstract: A thrust estimation scheme for a marine propeller has been experimentally tested in waves and with a device that simulates the influence of a vessel hull. The scheme is formed by a nonlinear propeller torque observer and a mapping to generate the thrust from the observed torque. The mapping includes the estimation of the advance number. This is utilized to improve the performance when the propeller is lightly loaded. The advance speed is assumed to be unknown, and only measurements of shaft speed and motor torque have been used. Accurate results have been obtained in experimental tests.

Keywords: Propulsion, state estimation, nonlinear, observers

## 1. INTRODUCTION

In the design of vessel control systems, such as Dynamic Positioning (DP), thruster assisted Position Mooring (PM) and autopilot systems, much effort has been put into the high-level control schemes. More recently, also the issue of local thruster dynamics and control has received more attention. For recent references, see for example Bachmayer *et al.* (Jan. 2000), Blanke *et al.* (2000), Whitcomb and Yoerger (1999), Sørensen and Smogeli (2006), Smogeli (2006) and references therein. The ability to design a good control system is mainly limited by two difficulties: to model the vessel's and the propeller's dynamics and to measure the environmental state. For example in severe weather conditions high thrust losses due to ventilation, in-and-out-of water effects and wave-induced water velocities are experienced. There are also losses of thrust due to the interaction between the vessel hull and the propeller. Recently, observers for monitoring the propeller performance have been developed and included in new control designs for electrically driven propellers, see Guibert *et al.* (2005) and Smogeli (2006).

All these considerations motivate the development of schemes to estimate the propeller thrust because, in general, its measurement is not available. The incorporation of the estimated thrust in a controller could improve the overall control performance. Moreover the performance monitoring will also be important for improving thrust allocation in different working conditions of the propeller, from normal to extreme environmental operating conditions.

The problem of the propeller thrust estimation has been treated in Zhinkin (1989) where full-scale experimental results were provided for positive shaft speed and vessel speed in steady-state conditions, in waves, and for slanted inflow. The estimation was based on the propeller torque measurement and on a linear relation between thrust and torque.

Thrust estimation has been also treated in Guibert *et al.* (2005), where the estimate was computed from the propeller torque obtained with a Kalman filter where a linear shaft friction torque was considered. The relation between thrust and torque involved an axial flow velocity model and requires the knowledge of the advance speed, very difficult

to measure in real vessel. The scheme was also highly sensitive to hydrodynamic and mechanical modelling errors. The results were presented in a simulation.

In Pivano *et al.* (2006a) a thrust estimation scheme that works in the four-quadrant plane composed by the vessel speed and the propeller shaft speed was proposed. The scheme involved a nonlinear observer for the propeller torque and a piecewise linear mapping to generate the propeller thrust from the observed torque. Accurate results were presented in Pivano *et al.* (2006a) for open water tests with the propeller deeply submerged. In this paper the scheme presented in Pivano *et al.* (2006a) is considered and experimentally tested under different conditions. The mapping to compute the thrust from the propeller torque has been improved in order to increase the accuracy when the propeller is lightly loaded. Differently from Guibert *et al.* (2005) the advance speed is assumed to be unknown. The scheme has been tested in waves to reproduce rough sea conditions and with a device that simulates the influence of a vessel hull. Results show that the estimation scheme provides good estimates in both conditions.

## 2. PROPELLER MODELING

A block diagram that represents the system is shown in Fig. 1.

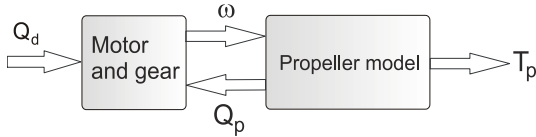


Fig. 1. Propeller system block diagram.

The shaft dynamics is derived by considering an electric motor attached to a shaft influenced by friction. It can be written as:

$$J_m \dot{\omega} = Q_m - Q_p - Q_f(\omega) \quad (1)$$

where  $J_m$  is shaft moment of inertia and  $Q_f$  is the shaft friction torque which depends on the shaft speed. In this paper it will be considered as a Coulomb plus a linear and nonlinear viscous effect:

$$Q_f(\omega) = k_{f_1} \arctan\left(\frac{\omega}{\epsilon}\right) + k_{f_2} \omega + k_{f_3} \arctan(k_{f_4} \omega) \quad (2)$$

This is motivated by the experimental result of the system identification on the shaft friction torque for the propeller used for the experiments regarded in this paper (Pivano *et al.*, 2006b). In order to avoid the singularity in zero, the Coulomb effect, usually written as a  $\text{sign}(\omega)$ , has been replaced by the function  $\arctan(\frac{\omega}{\epsilon})$  with a small positive  $\epsilon$ . All the coefficients  $k_{f_i}$  are constant and positive.

## 3. THRUST ESTIMATION SCHEME

The scheme implemented to derive the propeller thrust is shown in the block diagram of Fig. 2. The propeller shaft speed  $\omega$  and the motor torque  $Q_m$  are assumed to be measurable. First a stable observer is designed to estimate the propeller load torque  $Q_p$ . Second, an estimate of the propeller thrust  $T_p$  is computed from the estimated propeller torque.

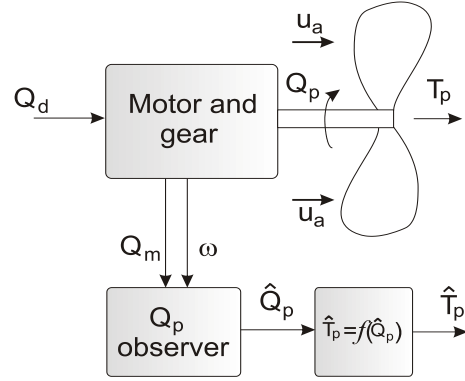


Fig. 2. Propeller thrust estimation scheme.

### 3.1 Propeller torque observer

To derive a stable observer for the propeller torque the following system is considered (Pivano *et al.*, 2006a):

$$J_m \dot{\omega} = Q_m - Q_p - Q_f(\omega) + \Delta_f \quad (3)$$

$$\dot{Q}_p = -\frac{1}{\tau_q} Q_p + w_q \quad (4)$$

where the propeller torque  $Q_p$  is treated as a time-varying parameter and modeled as a first order process with positive time constant  $\tau_q$  and driven by a bounded random noise  $w_q$ . In (3) a friction modeling error and measurement error on  $Q_m$  are accounted for by  $\Delta_f$ . The following observer with gains  $L_1$  and  $L_2$  is proposed:

$$J_m \dot{\hat{\omega}} = Q_m - \hat{Q}_p - Q_f(\hat{\omega}) + L_1(y - \hat{y}) \quad (5)$$

$$\dot{\hat{Q}}_p = -\frac{1}{\tau_q} \hat{Q}_p + L_2(y - \hat{y}) \quad (6)$$

The measurement

$$y = \omega + v \quad (7)$$

is assumed to be corrupted by an error  $v$ . We assumed that  $\Delta_f$ ,  $v$  and  $w_q$  are bounded. With  $\tilde{x}_1 = \omega - \hat{\omega} = x_1 - \hat{x}_1$  and  $\tilde{x}_2 = Q_p - \hat{Q}_p = x_2 - \hat{x}_2$ , the error dynamics can be written as:

$$\begin{aligned} \dot{\hat{x}}_1 = & \frac{1}{J_m} \left[ -\tilde{x}_2 - k_{f_1} \left( \arctan \left( \frac{x_1}{\epsilon} \right) - \arctan \left( \frac{\hat{x}_1}{\epsilon} \right) \right) \right] \\ & + \frac{1}{J_m} [-k_{f_3} (\arctan(k_{f_4} x_1) - \arctan(k_{f_4} \hat{x}_1))] \\ & + \frac{1}{J_m} [-k_{f_2} \tilde{x}_1 - L_1 \tilde{x}_1 + \Delta_f - L_1 v] \end{aligned} \quad (8)$$

$$\dot{\hat{x}}_2 = -\frac{1}{\tau_q} \tilde{x}_2 - L_2 \tilde{x}_1 - L_2 v + w_q \quad (9)$$

Noise and measurement errors can be treated as inputs, grouped in the vector  $u = [u_1 \ u_2 \ u_3] = [\Delta_f \ v \ w_q]^T$ .

*Proposition 1.* Suppose that the following assumptions are satisfied

$$\mathbf{A1} \quad L_1 > -k_{f_2}$$

$$\mathbf{A2} \quad \left| \frac{1}{J_m} + L_2 \right| < 2\sqrt{\frac{1}{\tau_q} \left( \frac{k_{f_2} + L_1}{J_m} \right)}.$$

Then the system of (8) and (9) is input-to-state stable (ISS) with respect  $u$ .

**Proof.** see Pivano *et al.* (2006a). ■

### 3.2 Thrust/torque relationship

The propeller thrust is closely related to the propeller torque and, in general, the relation is a nonlinear function. The results obtained from experimental test in Zhinkin (1989) showed that the relation between thrust and torque is very stable. This allows us to use the propeller torque, either measured or estimated, to compute the thrust when its measurement is not available. In Pivano *et al.* (2006a) it was shown that the relation between the propeller thrust and torque could be approximated with a linear piecewise function. The mapping showed good results on reproducing the thrust from the estimated propeller torque during various experimental tests. The linear relation between thrust and torque used in Pivano *et al.* (2006a) may not provide accurate results when the propeller is lightly loaded, i.e. working at high values of the advance number  $J$ , as explained later. The advance number  $J$  is computed as:

$$J = \frac{2\pi u_a}{\omega D}$$

where  $D$  is the propeller disc diameter and  $u_a$  is the advance speed (the ambient inflow velocity of the water to the propeller). The advance speed is difficult to measure on real vessels and is normally different from the vessel speed due to the interaction between the vessel hull and the propeller. To relate the thrust and torque, the standard propeller characteristics  $K_T$  and  $K_Q$  are considered. From Van Lammeren *et al.* (1969) we have:

$$T_p = K_T \frac{\rho \omega^2 D^4}{4\pi^2} \quad (10)$$

$$Q_p = \frac{K_Q \rho \omega^2 D^5}{4\pi^2} \quad (11)$$

Fig. 3 shows the measured propeller characteristics of the propeller considered in this paper.

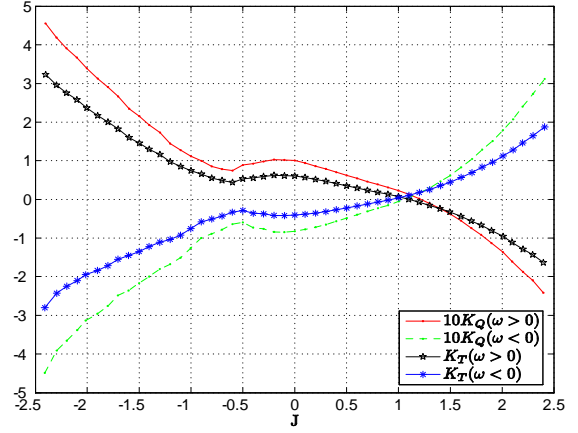


Fig. 3. Propeller characteristics  $K_T$  and  $K_Q$ .

Fig. 4 (b) shows the ratio between the propeller thrust and torque for positive shaft speed  $\omega$  computed from the propeller characteristics of Fig. 3 as:

$$\frac{T_p}{Q_p} = \frac{K_T}{K_Q D} \quad (12)$$

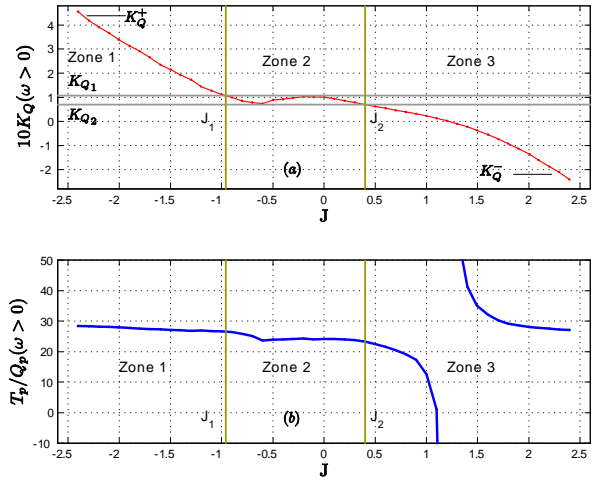


Fig. 4.  $K_Q$  characteristic and the ratio between thrust and torque for  $\omega > 0$ .

In Fig. 4 (b) we can see that for values of  $J$  greater than  $J_2$ , the thrust and torque ratio changes substantially and to compute accurately the thrust from the torque, the values of  $J$  need to be known. The procedure employed to estimate the thrust from the propeller torque is summarized in the following steps:

- Computation of  $\hat{K}_Q$ , an estimate of  $K_Q$ , solving (11) where  $\hat{Q}_p$  is used instead of  $Q_p$ . From Fig. 4 we can also see that for values of  $K_Q$  outside the region limited by  $K_Q^+$  and  $K_Q^-$ , the ratio between thrust and torque is

basically constant. For this reason the value of  $\hat{K}_Q$  can be set to be equal to  $K_Q^+$  when  $\hat{K}_Q$  computed with (11) is greater than  $K_Q^+$  and set to  $K_Q^-$  if  $\hat{K}_Q$  is less than  $K_Q^-$ .

- Calculation of  $\hat{J}$ , an estimate of the advance number  $J$ , inverting the  $K_Q$  curve using the calculated  $\hat{K}_Q$ . From Fig. 4 (a) we can see that it is not possible to obtain exactly the value of  $J$  around zero because the  $K_Q$  curve in not invertible. To solve this problem the  $J$  axis has been divided in three zones as shown in Fig. 4. In the zone 1 ( $J < J_1$ ) and zone 3 ( $J > J_2$ ) the  $K_Q$  curve is invertible and  $J$  can be find accurately. When  $K_{Q_2} \leq K_Q \leq K_{Q_1}$  (zone 2) we approximate  $\hat{J}$  with zero. Since in zone 2 the ratio between thrust and torque does not change considerably, this approximation introduces a small error in the overall mapping.
- Computation of  $\hat{K}_T$ , an estimate of  $K_T$ , using the propeller characteristics and  $\hat{J}$ .
- Calculation of the thrust with (10) where  $\hat{K}_T$  is used instead of  $K_T$ .

A block diagram that shows the procedure is presented in Fig. 5.

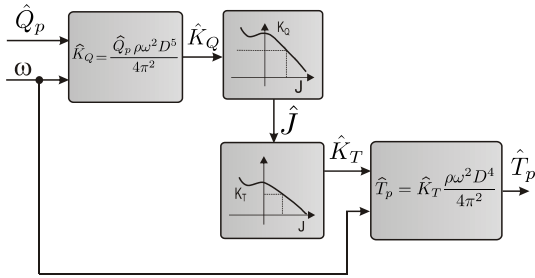


Fig. 5. Thrust estimation block diagram.

## 4. EXPERIMENTAL RESULTS

### 4.1 Setup

The experiments were performed at the MCLab ( [www.itk.ntnu.no/marinkyb/MCLab/](http://www.itk.ntnu.no/marinkyb/MCLab/) ), an experimental laboratory located at NTNU (Trondheim, Norway). The basin, 6.45m wide, 40m long and 1.5m deep, is equipped with a 6DOF towing carriage that can reach a maximum speed of 2m/s and with a wave generator able to generate waves up to 30cm.

The tests have been performed on a four bladed propeller with a diameter of 25cm. A metallic grid has been placed upstream of the propeller in order to reduce the speed of the inflow to the propeller disc. In this way we could simulate the presence of the vessel hull. A sketch of the setup is shown in Fig. 6.

Some tests were performed in order to measure the standard propeller characteristics shown in Fig. 3 and to measure the four-quadrant propeller

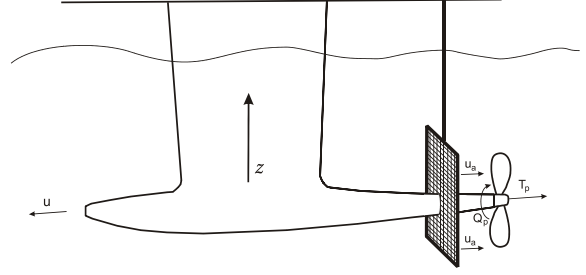


Fig. 6. Sketch of the experimental setup.

characteristic, the  $C_T$  and  $C_Q$  coefficients plotted as a function of the advance angle  $\beta$ . The advance angle  $\beta$  is computed with the four quadrant inverse tangent function as:

$$\beta = \arctan2(u_a, 0.7R\omega) \quad (13)$$

where  $R$  is the propeller disc radius. The thrust and torque coefficients are computed from Van Lammeren *et al.* (1969) as:

$$C_T = \frac{T_p}{\frac{1}{2}\rho V_r^2 A_0} \quad (14)$$

$$C_Q = \frac{Q_p}{\frac{1}{2}\rho V_r^2 A_0 D} \quad (15)$$

where  $A_0$  is the propeller disc area,  $\rho$  is the water density,  $D$  is the propeller diameter and  $V_r$  is the relative advance velocity:

$$V_r^2 = u_a^2 + (0.7R\omega)^2 \quad (16)$$

The four quadrant characteristics of to the propeller considered in this paper is shown in Fig. 7.

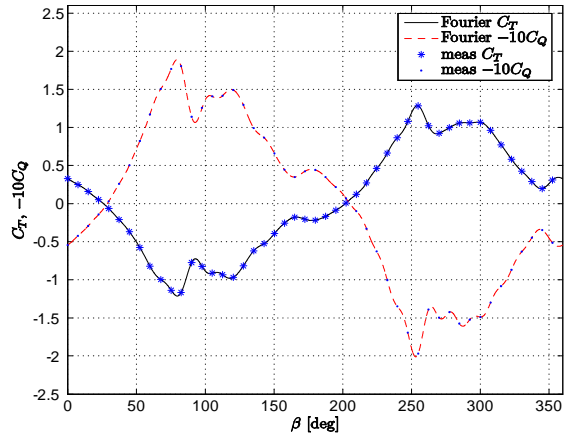


Fig. 7. Propeller four-quadrant open water characteristics.

Some tests were performed with different profiles of vessel speed and various types of motor torque: square, sinusoidal and triangular waves of different amplitudes and frequencies. This was done using the built-in torque controller of the motor driver. Other tests have been performed using the built-in velocity controller enabling control of the propeller shaft speed. To perform tests in rough sea conditions, regular waves of 20cm amplitude

have been generated with the wave maker. At the same time the propeller was moving in a sinusoidal vertical motion to simulate the vertical oscillation that occurs in rough sea due to vessel motion and waves.

#### 4.2 Friction Torque

The friction torque has been modeled as the static function of (2). Fig. 8 shows the friction torque computed from measurements and the model which has been used in the observer. For the propeller tested, the losses due to the friction torque are quite high compare to a full scale propeller, where losses are usually less than 6%.

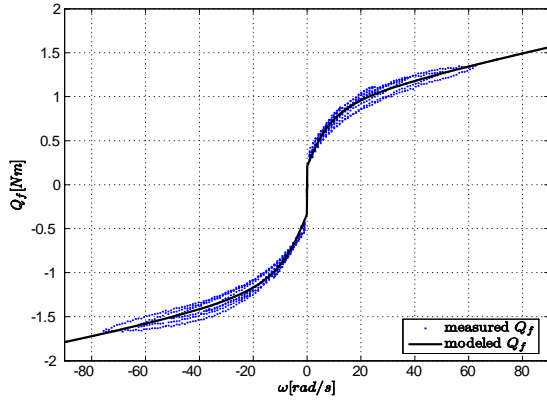


Fig. 8. Friction torque: computed from measurements and a static approximation.

#### 4.3 Results

The thrust estimation scheme has been validated with the observer gains  $L_1$  and  $L_2$  reported in Table 1.

Fig. 9 shows results from a test where the speed of the vessel varies from 1m/s to -1m/s while the shaft speed assumes positive and negative values. Both the estimated thrust  $\hat{T}_p$  and torque  $\hat{Q}_p$  are very accurate. In Fig. 9 the thrust computed through (13), (14) and (16) with the four-quadrant characteristic  $C_T$  depicted in Fig. 7 is reported. In (16) the speed of the vessel  $u$  has been used instead of the unknown advance speed  $u_a$ . When the vessel speed is positive the computed thrust is lower than the measured one because, due to the metallic grid, the advance speed is lower than the vessel speed. When the vessel speed is negative, the thrust computed with the propeller characteristic is about the average of the measured thrust because the advance speed is equal to vessel speed. When the vessel travels backwards the inlet water flow is not affected by the grid which is placed upstream of the propeller.

Fig. 10 shows the result of a test performed in regular waves with height 20cm and the propeller moved along its vertical axis with a sinusoidal

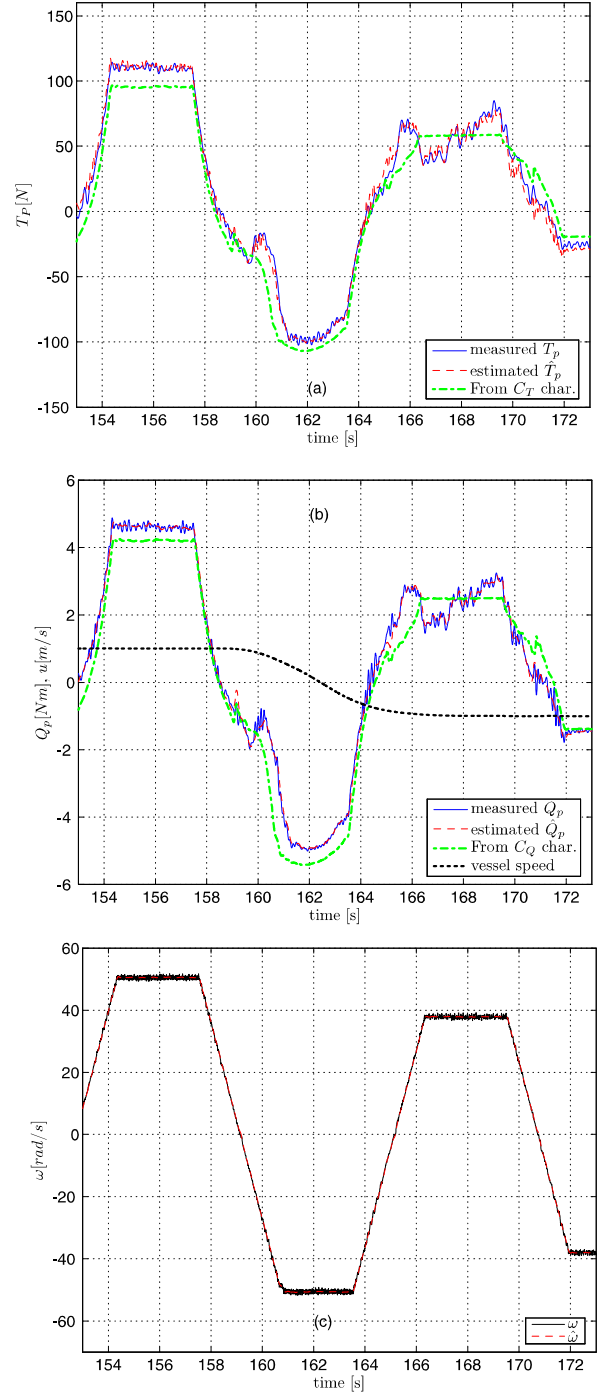


Fig. 9. Experimental results with the vessel in motion.

motion. Fig. 10 (c) shows the vertical displacement along the propeller vertical axis that points upwards as shown in Fig. 6. The propeller shaft speed has been kept constant at 38rad/s. A drop of thrust and torque occurs when the propeller rotates close to the water surface since the load decreases due to ventilation. The oscillations of torque, due to waves that disturb the inflow to the propeller are well reproduced by the estimate. The estimated thrust is not as accurate as for the test without waves but the drop is properly captured and the estimation error is small. The results show that even in this extreme case, the estimates provided are quite accurate.

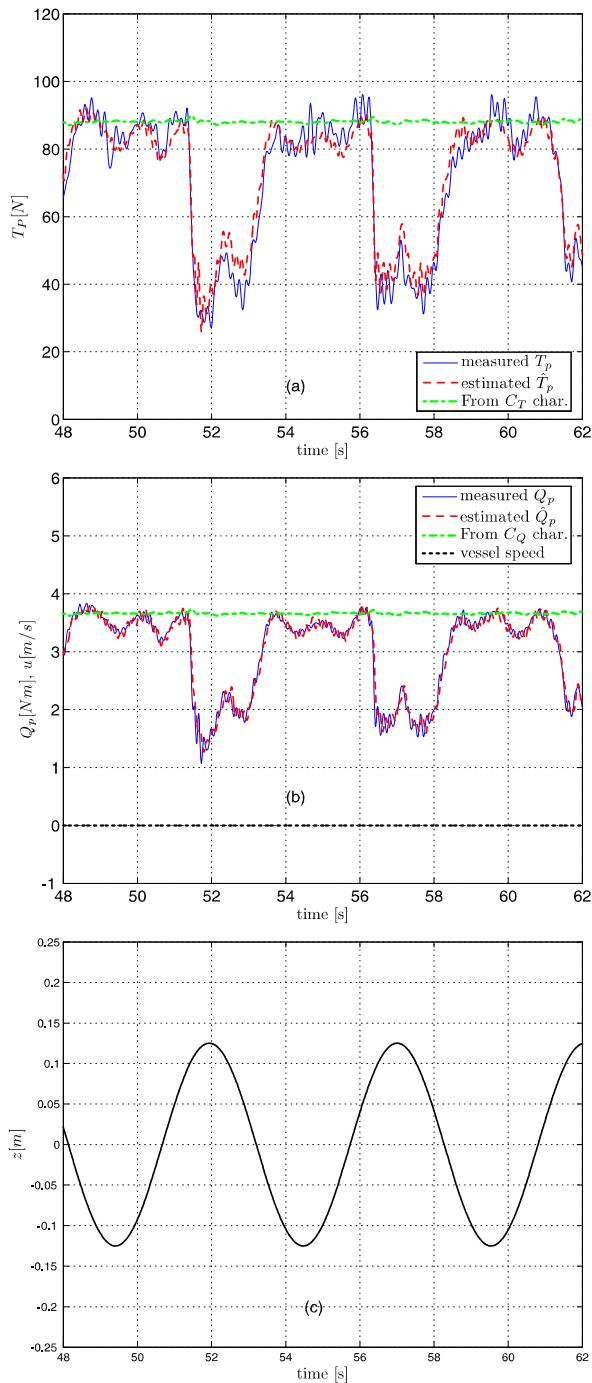


Fig. 10. Experimental results with waves and constant shaft speed.

Table 1. Observer parameters

Parameter	Value	Parameter	Value
$J_m [Kg m^2]$	$5.84 \cdot 10^{-3}$	$\epsilon$	$1 \cdot 10^{-6}$
$k_{f1}$	$1.8 \cdot 10^{-2}$	$\tau_Q [s]$	10
$k_{f2}$	$1.29 \cdot 10^{-2}$	$L_1$	3.5
$k_{f3}$	$6.96 \cdot 10^{-1}$	$L_2$	$-1/J_m$
$k_{f4}$	$8.03 \cdot 10^{-1}$		

## 5. CONCLUSION

In this paper, a thrust estimation scheme for marine propellers has been experimentally tested in waves to reproduce rough sea conditions and with

a device that simulates the presence of a vessel hull. The scheme includes a nonlinear observer to estimate the propeller torque and a mapping to compute the thrust from the observed torque. The advance speed is assumed to be unknown and only measurements of shaft speed and motor torque have been used. Experimental results show the good performances of the proposed scheme.

## 6. ACKNOWLEDGMENT

The authors acknowledge Professor Sverre Steen for valuable suggestions and discussions. The Norwegian Research Council is acknowledged as the main sponsor of this project.

## REFERENCES

- Bachmayer, R., L. L. Whitcomb and M. A. Grosenbaugh (Jan. 2000). An accurate four-quadrant nonlinear dynamical model for marine thrusters: Theory and experimental validation. *IEEE J. Oceanic Eng.* **25**, 146–159.
- Blanke, M., K. Lindegaard and T. I. Fossen (2000). Dynamic model for thrust generation of marine propellers. *5th IFAC Conference of Manoeuvring and Control of Marine craft, MCMC* pp. 363–368.
- Guibert, C., E. Foulon, N. Ait-Ahmed and L. Loron (2005). Thrust control of electric marine thrusters. *Industrial Electronics Society. IECON 2005. 32nd Annual Conference of IEEE*.
- Pivano, L., Ø. N. Smogeli, T. A. Johansen and T. I. Fossen (2006a). Marine propeller thrust estimation in four-quadrant operations. *To appear in the 45th IEEE Conference on Decision and Control, San Diego, CA, USA*.
- Pivano, L., T. I. Fossen and T. A. Johansen (2006b). Nonlinear model identification of a marine propeller over four-quadrant operations. *14th IFAC Symposium on System Identification, SYSID, Newcastle, Australia*.
- Smogeli, Ø. N. (2006). Propulsion Control: from Normal to Extreme Conditions. PhD thesis. Department of Marine Technology, Norwegian University of Science and Technology (NTNU). Trondheim, Norway. To be published.
- Sørensen, A. J. and Ø. N. Smogeli (2006). Torque and power control of electrically driven propellers on ships. *Accepted for publication in the IEEE Journal of Oceanic Engineering*.
- Van Lammeren, W. P. A., J. D. Van Manen and M. W. C. Oosterveld (1969). The Wageningen B-Screw Series. *Transactions of SNAME*.
- Whitcomb, L. L. and D. Yoerger (1999). Development, comparison, and preliminary experimental validation of nonlinear dynamic thruster models. *IEEE/MTS Ocean Eng.* **24**, 481–494.
- Zhinkin, V. B. (1989). Determination of the screw propeller thrust when the torque or shaft power is known. *Fourth international symposium on practical design of ships and mobile units, 23-38 October, Bulgaria*.